

exploration review

EXTRACTING MEANINGFUL INFORMATION FROM SEISMIC ATTRIBUTES

Satinder Chopra, Arcis Corporation, Calgary

Seismic attributes are a powerful aid to seismic interpretation. They allow the geoscientist to interpret faults and channels, recognize the depositional environment, and unravel the structural deformation history more rapidly. By combining information from adjacent seismic samples and traces using a physical model (such as dip and azimuth, waveform similarity, or frequency content), seismic attributes often organize features into displays that provide enhanced images for either a human interpreter or for modern geostatistical or neural-network computer analysis. While attributes are sensitive to lateral changes in geology, they are also sensitive to lateral changes in noise. Seismic data are usually contaminated by both random and coherent noise, even when the data have been migrated reasonably well and are multiple free. Certain types of noise can be addressed by the interpreter through careful structure-oriented filtering or post-stack footprint suppression. While seismic attributes are particularly effective at extracting subtle features from relatively noise-free data, if the data are contaminated with multiples or are poorly focused and imaged due to poor statics or inaccurate velocities, the data will need to go back to the processing team to alleviate those problems.



Photo Overleaf

Low Impact Seismic (LIS) drilling rig completing a shot hole on a 3D project, along slopes of a sensitive area in south-central Saskatchewan.

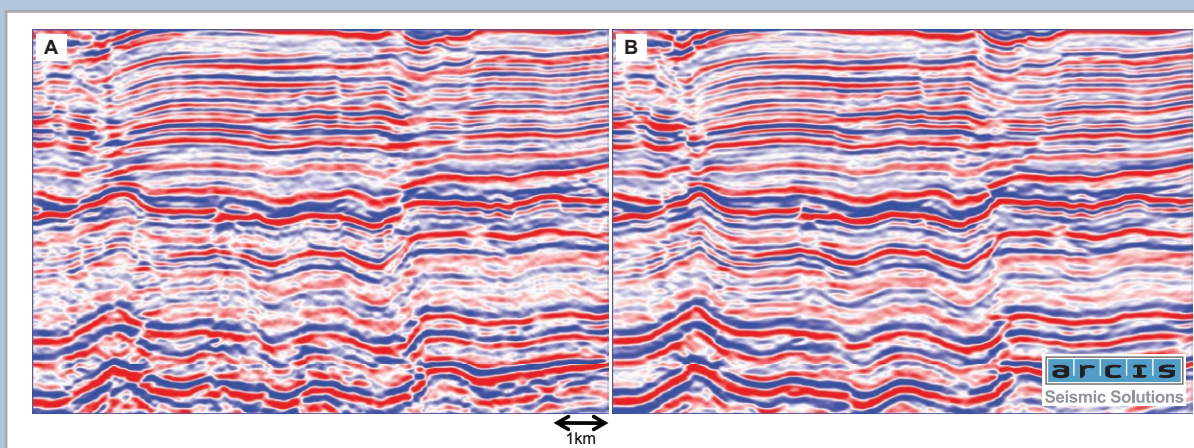
Photo Courtesy of ARCIS

Another common problem with seismic data is their relatively low bandwidth. Significant efforts are made during processing to enhance the frequency content of the data as much as possible to provide a spectral response that is consistent with the acquisition parameters. Since they are often unfamiliar with the targets of interest, the processors can be either too aggressive or too conservative in their filtering. In contrast, the interpreters will have a better understanding of the geology, the play concept, access to any well data, and therefore be better able to keep or reject alternative filter products that are consistent or inconsistent with the interpretation hypothesis. In this paper, alternative means of suppressing random noise on our migrated seismic images are discussed, and then acquisition footprint, which may appear to be random in the temporal domain, but is highly correlated to the acquisition geometry in the spatial domain is addressed. After passing the data through the cleaning phase, alternative methods for frequency enhancement of the input seismic data are evaluated. Next, the impact of attributes such as coherence and curvature on data volumes from Alberta, Canada is illustrated. This review concludes with a summary of fre-

quency-enhancement methods based on these and other case study examples.

Alternative Noise-Suppression Workflows

Before discussing noise suppression workflows, one significant point is in order. That is, the seismic data being interpreted should be at least pre-stack migrated. A comparison of sections from post-stack and pre-stack migrated data volumes is shown in Figure 1 (► below). That figure depicts better sharpness of the faults and the coherency of the reflections with respect to the pre-stack data. Though a large fraction of the seismic data put through interpretation these days is pre-stack migrated, one must emphasize the importance of this process. Figure 2 (► opposite page) shows a comparison of time slices from the post and pre-stack time migrated volumes, and again, one can get a sense of better migration of reflection events on pre-stack migrated data. Notice the green arrows indicating the clarity with which the faults are imaged, as well as the definition of the individual red or blue blobs seen on the time slice from the pre-stack migrated data.



Segments of seismic inlines from 3D seismic volumes that are (A) post-stack migrated, and (B) pre-stack migrated. Notice the clarity of fault imaging and the coherence of the reflections.



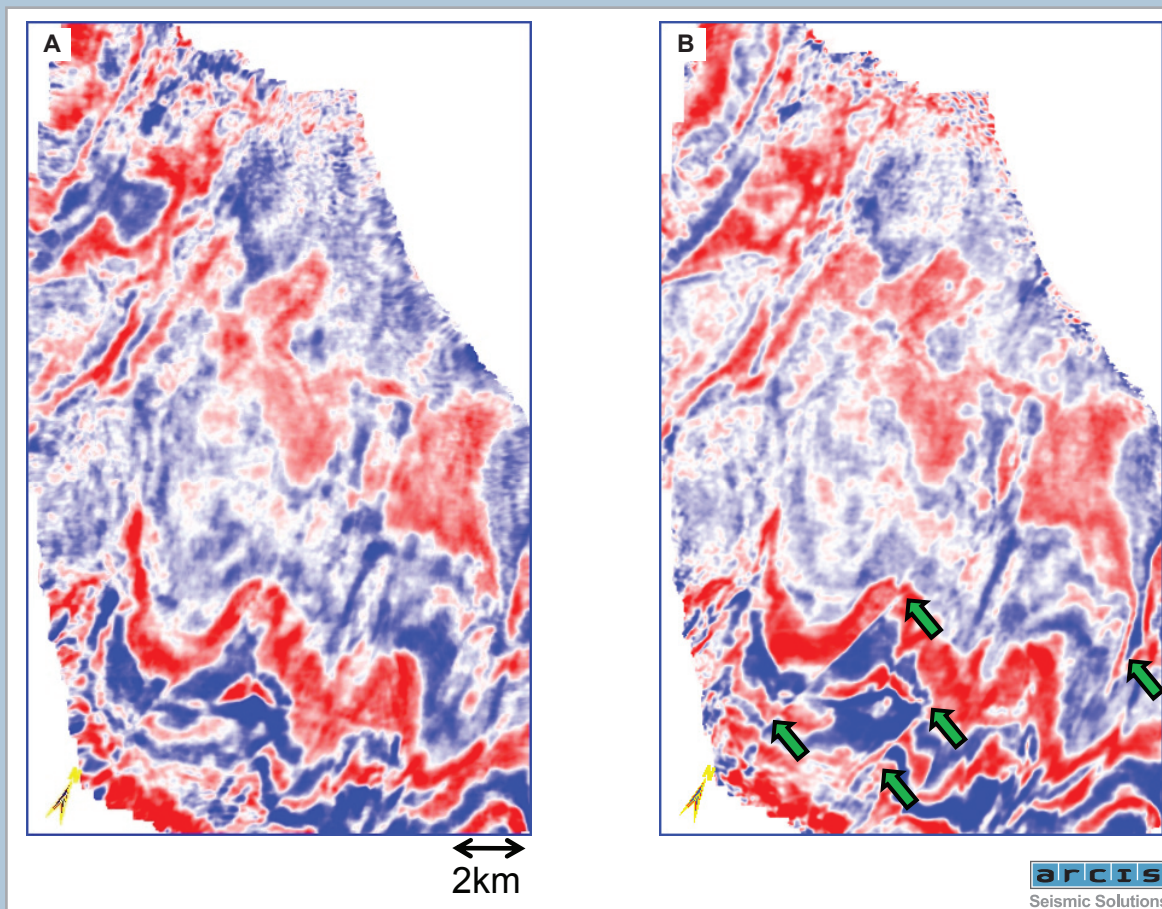
FIGURE 1: COMPARISON: POST-STACK VERSUS PRE-STACK IMAGING

From ARCIS

Data imaged accurately is likely to yield better results on the attribute volumes.

Suppression of random noise: Mean, alpha-trimmed mean, and median filters are commonly used during processing to suppress random noise. A more desirable application would be the application of a dip-steered mean or median filter, which has the effect of enhancing laterally continuous events by reducing randomly distributed noise without suppressing details in the reflection events consistent with the structure. The filter picks up samples within the chosen aperture along the local dip and azimuth and replaces the amplitude of the central sample position with the median value of the amplitudes. The median filter can also be applied iteratively, reducing random

noise at each successive iteration, but will not significantly increase the high frequency geological component of the surface (Chopra and Marfurt, 2008b). Dip-steered mean filters work well on pre-stack data in which discontinuities appear as smooth diffractions, but tend to smear faults and stratigraphic edges on migrated data. Dip-steered median and alpha-trimmed mean filters work somewhat better but will still smear faults. Hoecker and Fehmers (2002) address this problem through an “anisotropic diffusion” smoothing algorithm. The anisotropic part is so named because the smoothing takes place parallel to the reflector, while no smoothing takes place perpendicular to the reflector. The diffusion part of the name implies that the filter is applied iteratively, much as an interpreter would apply iterative



Time slices at 1610ms from 3D seismic volumes that are (A) post-stack migrated, and (B) pre-stack migrated. Notice the clarity of the fault imaging and the coherence of the reflection events seen in red and blue.

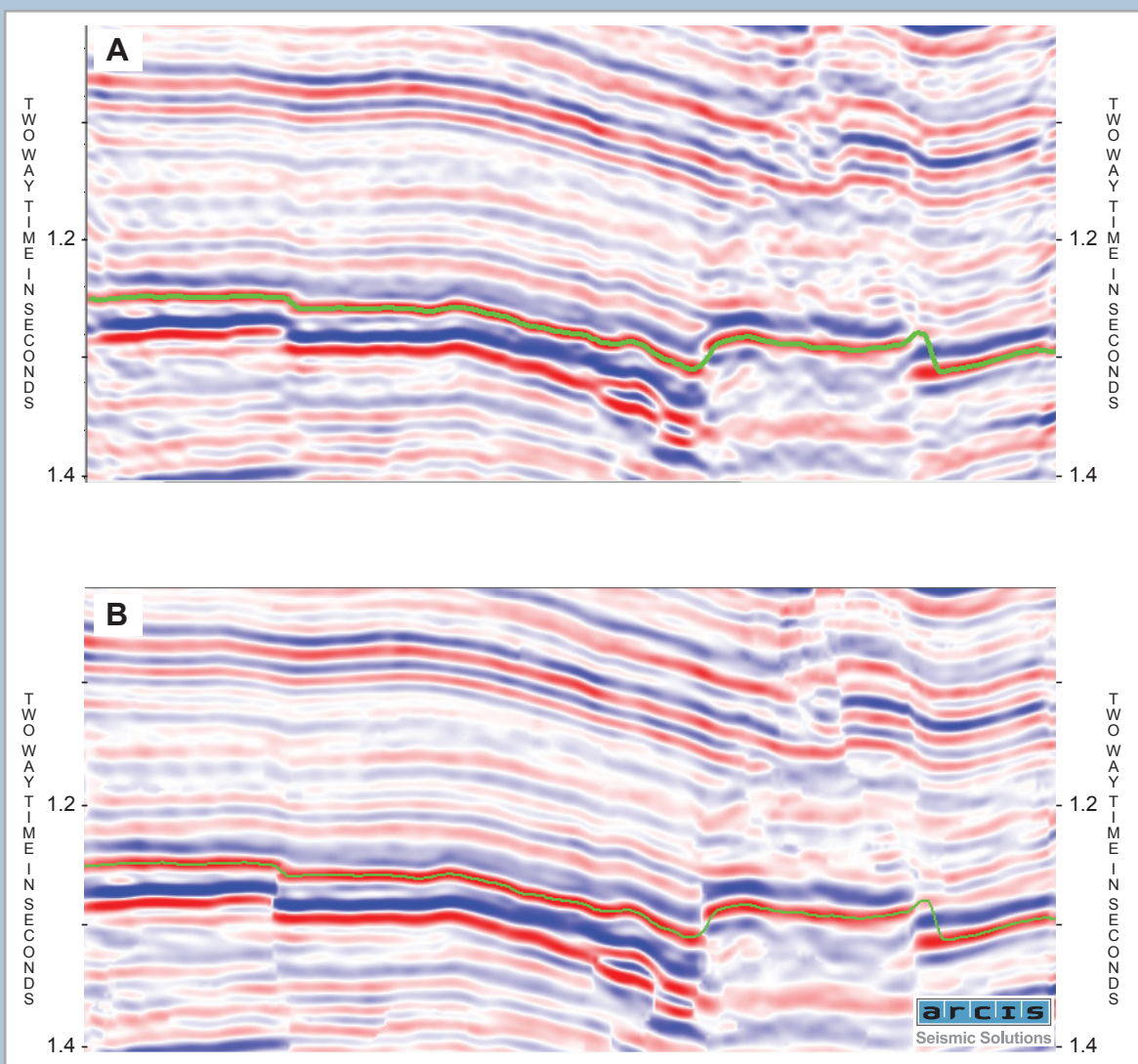


FIGURE 2: COMPARISON: POST-STOCK VERSUS PRE-STOCK IMAGING

From ARCIS

smoothing to a time structure map. Most important, no smoothing takes place if a discontinuity is detected, thereby preserving the appearance of major faults and stratigraphic edges. Luo et al. (2002) proposed a competing method that uses a multi-window (Kuwahara) filter to address the same problem. Both approaches use a mean or median filter applied to data values that fall within a spatial analysis window with a thickness of one sample. Marfurt (2006) describes a multi-window (Kuwahara) principal component filter that uses a small volume of data samples to compute the waveform

that best represents the seismic data in the spatial analysis window. Seismic processors may be more familiar with the principal component filter as equivalent to the Kohonen-Loeve (or simply KL) filter commonly used to model and remove multiples on NMO-corrected gathers using the multiple velocity. Examples of the application of structure-oriented filtering on seismic data have been shown in Chopra and Marfurt, (2007, 2008a), wherein improved event focusing and reduced background noise levels after structure-oriented filtering are clearly evident.

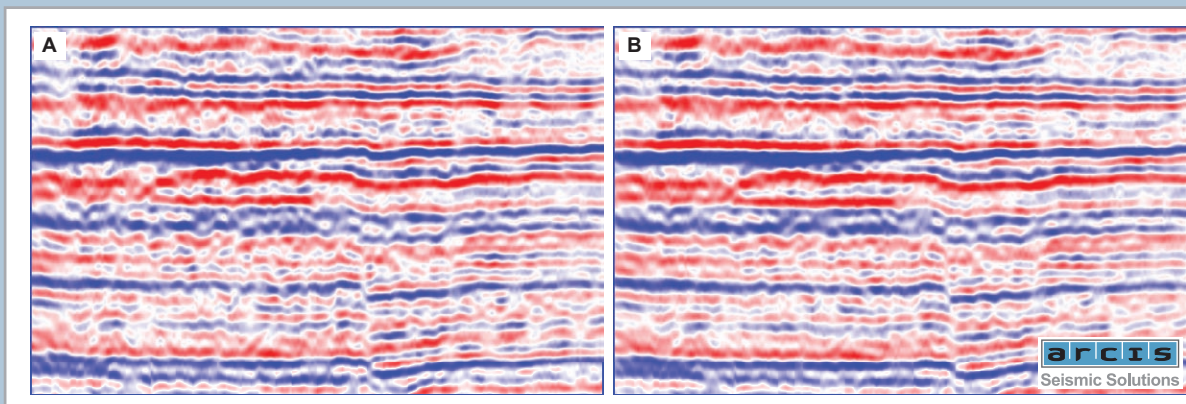


(A) An inline through the input data volume. (B) The same inline in (A), but after running structure-oriented filtering on the input data volume.



FIGURE 3: CONDITIONING OF DATA WITH STRUCTURE-ORIENTED FILTERING

From ARCIS



(A) An inline without footprint filtering (B) The same inline in (A), but after footprint filtering on the input data volume.



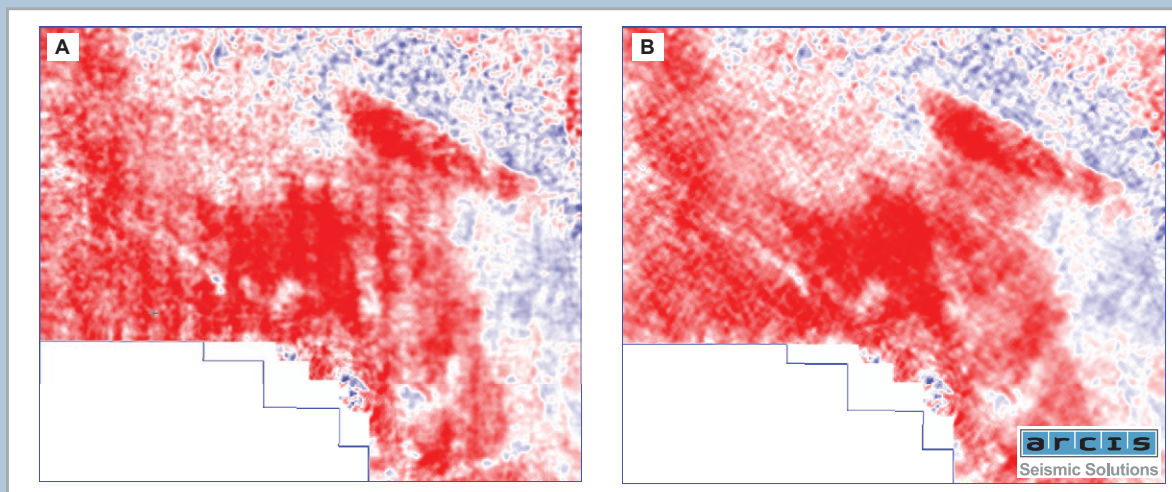
FIGURE 4: SUPPRESSION OF ACQUISITION FOOTPRINT

From ARCIS

Figure 3 (► below) shows a comparison of a segment of an inline before and after structure-oriented filtering on a seismic dataset. Figure 3A (► opposite page) is part of an inline through the input seismic volume, and figure 3B (► opposite page) is the same inline after structure-oriented filtering on the input data volume. Notice the cleaner

look of the section after filtering, as well as the sharpening of the vertical faults.

Suppression of acquisition footprint: Acquisition footprint is defined as any amplitude or phase anomaly closely correlated to the surface acquisition geometry rather than to the subsurface geology. Spatially periodic changes in total fold, azimuths

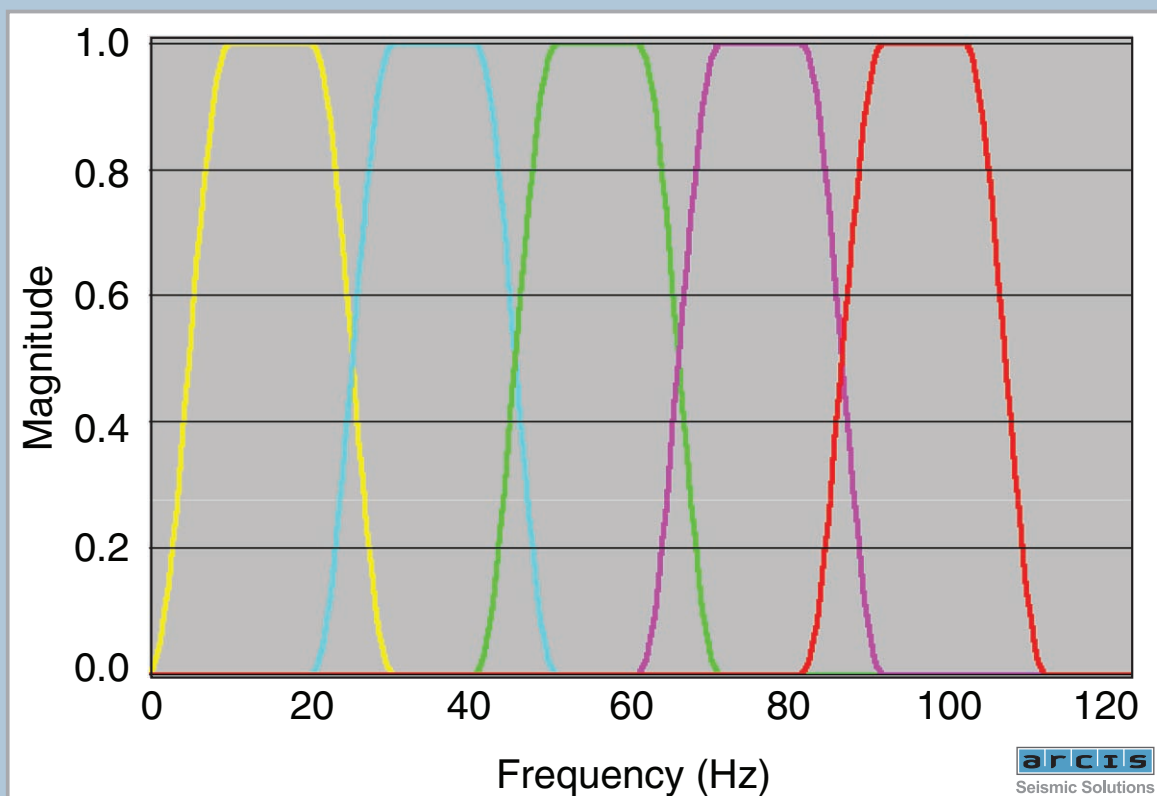


Time slices (769 ms) from data volumes (A) without footprint filtering, (B) after footprint filtering on the input data volume.



FIGURE 5: SUPPRESSION OF ACQUISITION FOOTPRINT

From ARCIS



In frequency-split structure-oriented filtering, the seismic data are first band-pass filtered such as the 5-pass band shown above. Each pass band is subsequently SOF-filtered along a consistent structural dip for noise attenuation. The results are normalized to the amplitude of the original spectrum and then added.



FIGURE 6: FREQUENCY-SPLIT STRUCTURE-ORIENTED FILTERING

From ARCIS

and offsets give rise to spatial periodicity in enhancement of seismic signal and rejection of seismic noise. Attributes exacerbate these periodic changes, giving rise to artifacts. Gulunay (2006) and others have shown that $kx-ky$ filters can be very effective in reducing acquisition footprint on time slices for regularly sampled surveys. Footprint due to fold, offset and azimuth tends to be organized vertically, while that due to aliased migration artifacts is steeply dipping, $kx-ky-\omega$ or 3D running-window. Radon filters may provide some additional artifact suppression leverage. For more irregular acquisition design, the noise estimated using $kx-ky$ or $kx-ky-\omega$ filters can be followed by an adaptive filter.

Figure 4 (► page 21) shows a comparison of a segment of a seismic section before and after footprint filtering. Notice that the footprint manifests on seismic data in the form of

amplitude variations along reflections and also gives them a somewhat chaotic look. The footprint-filtered section shows better coherency of reflections. Figure 5 (► page 21) shows a time slice comparison before and after footprint filtering. Again, notice the vertical imprint clearly masks the time slice (A), but the equivalent time slice after footprint filtering looks clearer (B).

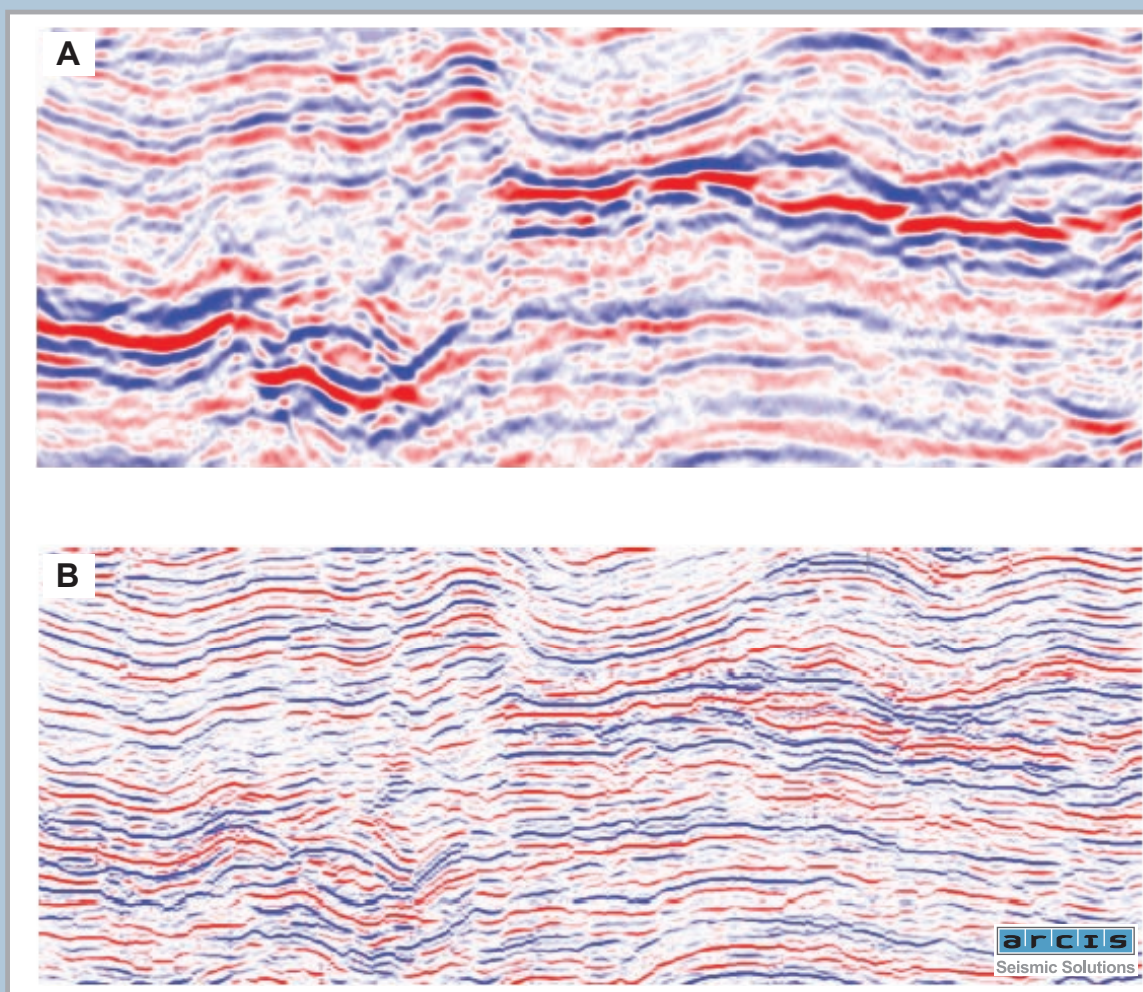
Enhancing the frequency bandwidth of seismic data

There are a number of methods that are used during processing to enhance the frequency content of the input seismic data. Here, a few commonly used processes followed by some relatively newer ones that help the interpreter to extract meaningful information from the seismic data are mentioned.

Deconvolution: Different conventional procedures are adopted to compensate for frequency attenuation. A common practice has been to use a two- or three-window statistical deconvolution to correct for the dynamic loss of high frequencies. This involves choosing two or three time windows for the deconvolution, each with its own parameters, keeping the time-variant nature of the embedded source wavelet in mind. These windows are usually designed to overlap in order to avoid artifacts. However, there are problems with this approach; the filters must be derived from smaller windows, which are less likely

to meet the statistical assumptions, and these windowed zones often exhibit phase distortions at the point of overlap.

Time-variant spectral whitening: The other method is to use time-variant spectral whitening (TVSW). This method involves passing the input data through a number of narrow band-pass filters and determining the decay rates for each frequency band. The inverse of these decay functions for each frequency band is applied, and the results are summed. In this way, the amplitude spectrum for the output data is whitened in a time-variant way. The number of filter

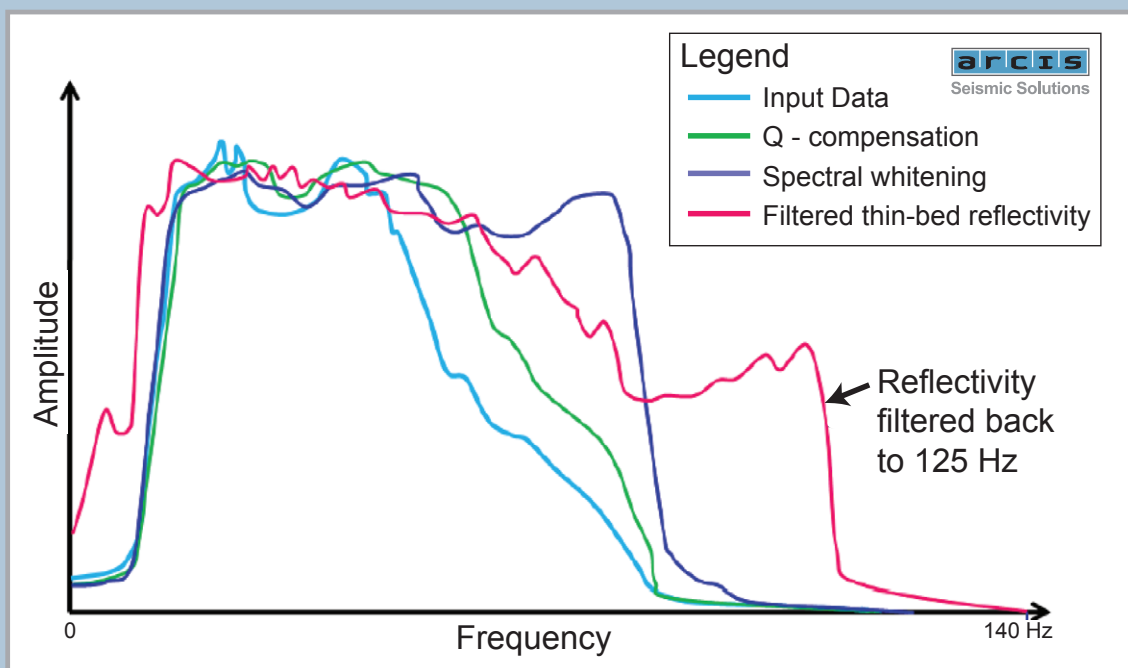


(A) A segment of a seismic section; (B) equivalent thin-bed reflectivity section derived from the input section. Notice the higher resolution as well the extra cycles that help the interpreter make more accurate interpretation.



FIGURE 7: EXTRACTION OF REFLECTIVITY

From ARCIS



Amplitude spectra of frequency-enhanced different datasets using Q-compensation, spectral whitening and filtered thin bed reflectivity. Since Q-compensation is model-based, it shows only a moderate increase in frequency content. Spectral whitening is statistically-based and provides a significantly greater increase in frequency content. Thin-bed reflectivity extends the spectrum using a sparse spike model. In this case, the high-end cutoff is set to 125 Hz. Such bandwidth extension is valid if the earth can be represented by a suite of constant impedance vs. gradational or more smoothly varying layers.



FIGURE 8: FREQUENCY SPECTRA COMPARISON

From ARCIS

bands, the width of each band and the overall bandwidth of application are the different parameters that are used and adjusted for an optimized result (Yilmaz 2001). In this method, the high-frequency noise is usually amplified, and so a band-pass filter must be applied to the resulting data. Since it is a trace-by-trace process, TVSW is not appropriate for AVO applications.

Inverse Q-filtering: If we had an analytic form for an attenuation function, it would then be easy to compensate for its effects. Thus, in practice, attempts are first made to estimate a Q-model for the subsurface. Inverse Q-filtering is then carried out, removing the time-variant wavelet effects by absorption and broadening the effective seismic bandwidth by correcting the loss of high-frequency signal as well as compensating for dispersion effects that rotate each spectral component by a different amount. These attempts have met with a varying

degree of success, depending on the assumptions used in the particular approach and how well they are met in practice.

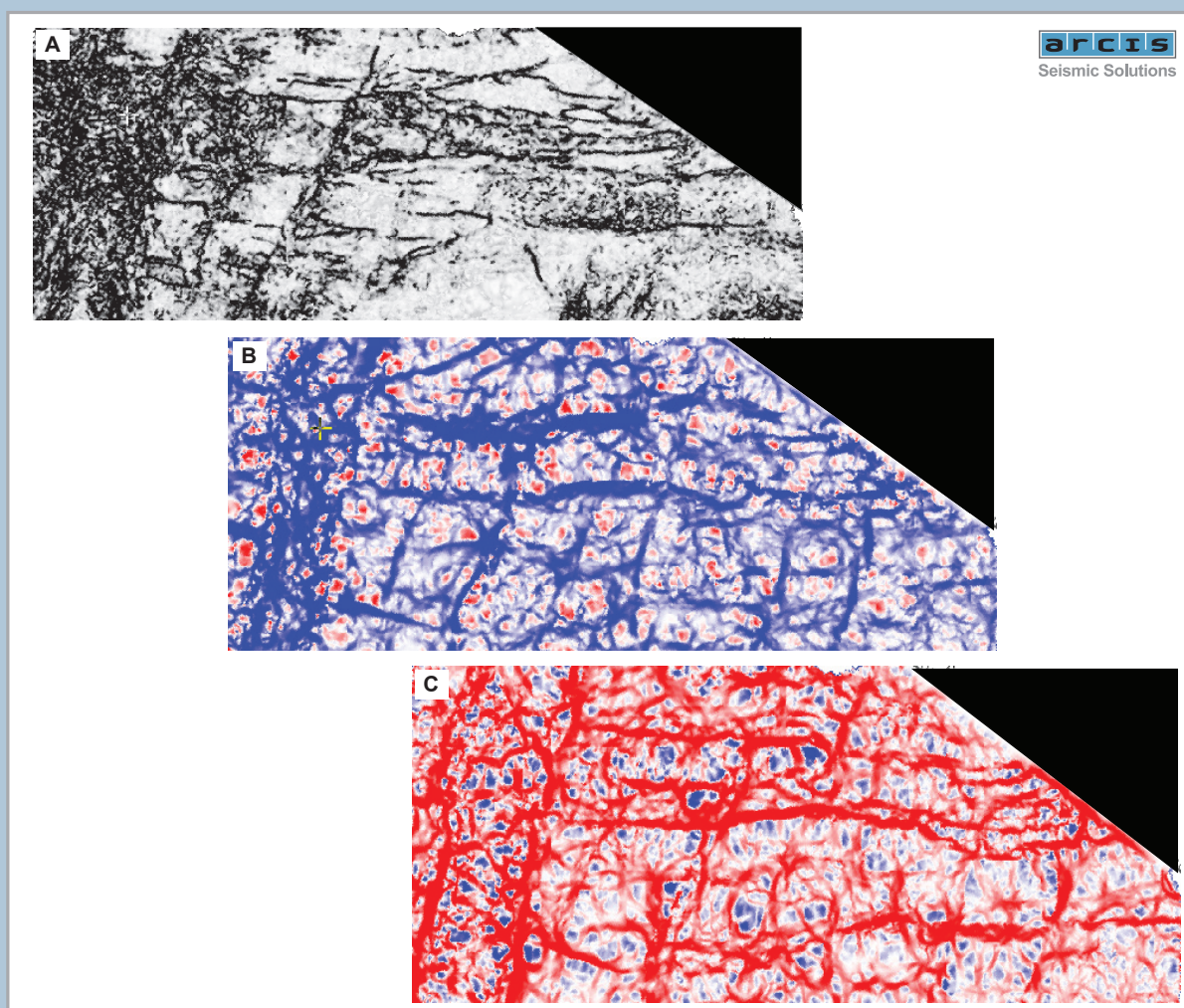
Frequency-split structurally-oriented filtering: Helmore (2009) introduced frequency-split structurally-oriented filtering (► figure page 22) wherein the input seismic data is divided into a number of frequency bands, followed by running structurally-oriented filters separately to each of the bands and then recombining the results. This procedure reduces noise in selected frequency bands and results in higher signal-to-noise ratio as well as enhanced resolution. Structurally oriented filters do not suffer from windowing artifacts and are precisely adapted to the local dip (Helmore, 2009).

Spectral decomposition-based inversion for seismic reflectivity: Thin-bed spectral inversion (Chopra et al., 2006) is a process that removes the time-variant wavelet from the seismic data

and extracts the reflectivity to image thicknesses far below seismic resolution using a matching pursuit implementation of sparse spike inversion. In addition to enhanced images of thin reservoirs, these frequency-enhanced reflectivity images have proven very useful in mapping subtle onlaps and offlaps, thereby facilitating the mapping of parasequences and the direction of sediment transport.

Figure 7 (▶ page 23) compares a segment of a 5–80 Hz seismic section from Alberta and its thin-bed reflectivity inversion. Notice the increased detail in terms of extra cycles.

It is convenient for an interpreter to convolve the derived reflectivity volume with a 5-120 Hz bandpass wavelet that would yield a high frequency volume. In addition to facilitating detailed interpretation, these ‘filtered’ volumes can serve as input for generating high-bandwidth attribute volumes. Figure 8 (▶ opposite page) shows the amplitude spectra for the same data volume subjected to the different methods discussed above. Notice that the high-frequency volume generated from thin-bed reflectivity inversion serves to show the highest frequency enhancement. Depending on the quality of the data as well as the access to one of the methods



Time slices from (A) coherence, (B) most-negative curvature and (C) most-positive curvature volumes. Notice the higher lineament detail on the curvature volumes as compared with coherence.



FIGURE 9: COHERENCE/CURVATURE ATTRIBUTE COMPARISON

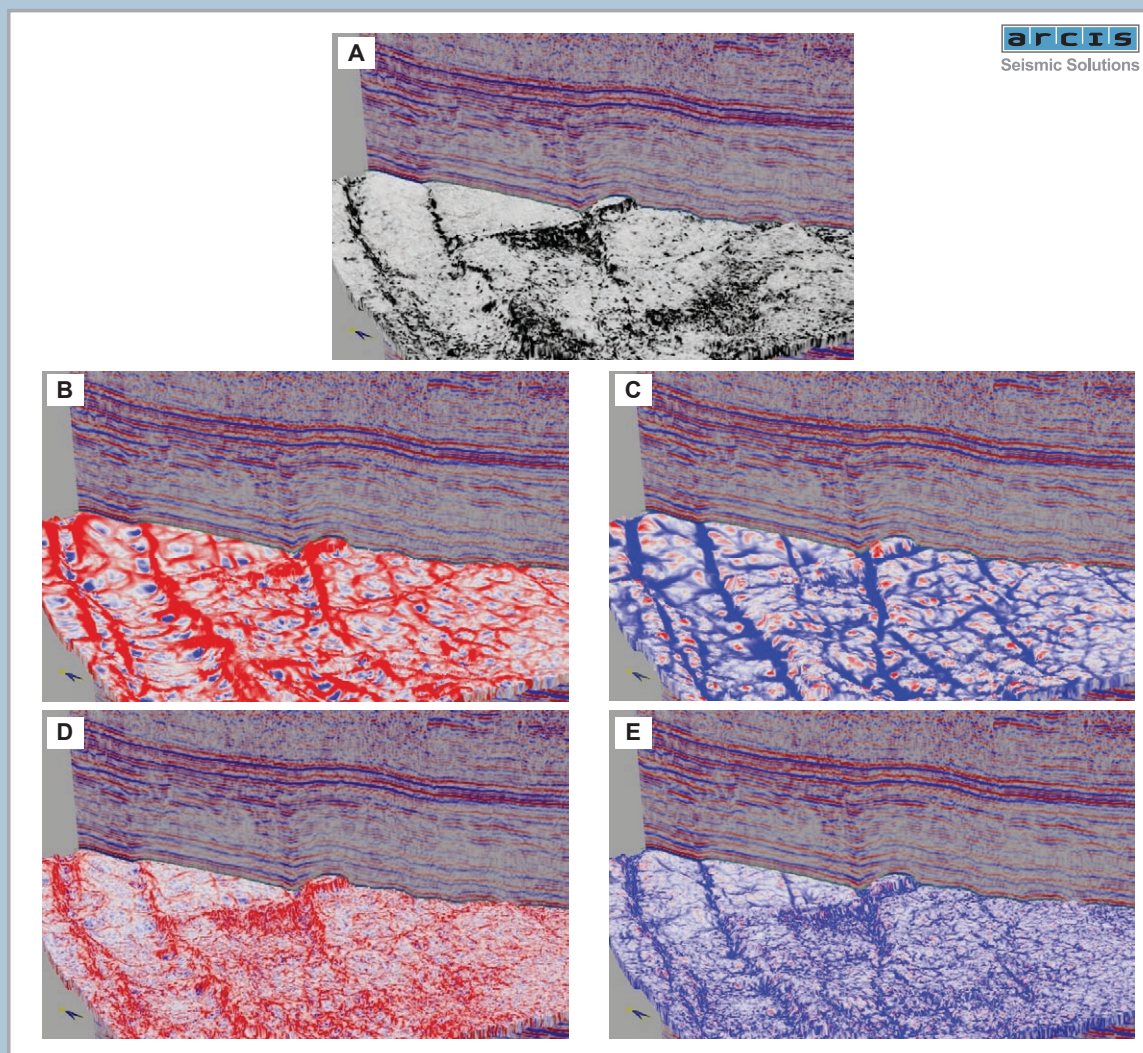
From ARCIS

discussed above, the data needs to be frequency-enhanced before the attributes can be computed effectively.

Benefits of attribute computation on preconditioned data

Two seismic discontinuity attributes that are commonly used for the determination of stratigraphic features as well as faults

and fractures are the coherence and curvature attributes. While coherence is a measure of similarity of adjacent seismic traces, curvature is a measure of the degree of bending of seismic reflections in the data. For volumetric computation of curvature, volumetric estimates of dip and azimuth are first computed using overlapping analysis windows (± 10 ms and nine traces for this discussion). Dip and azimuth computed in windows having a vertical extent are less sensitive to backscattered ground roll than calculating the dip and azimuth from the

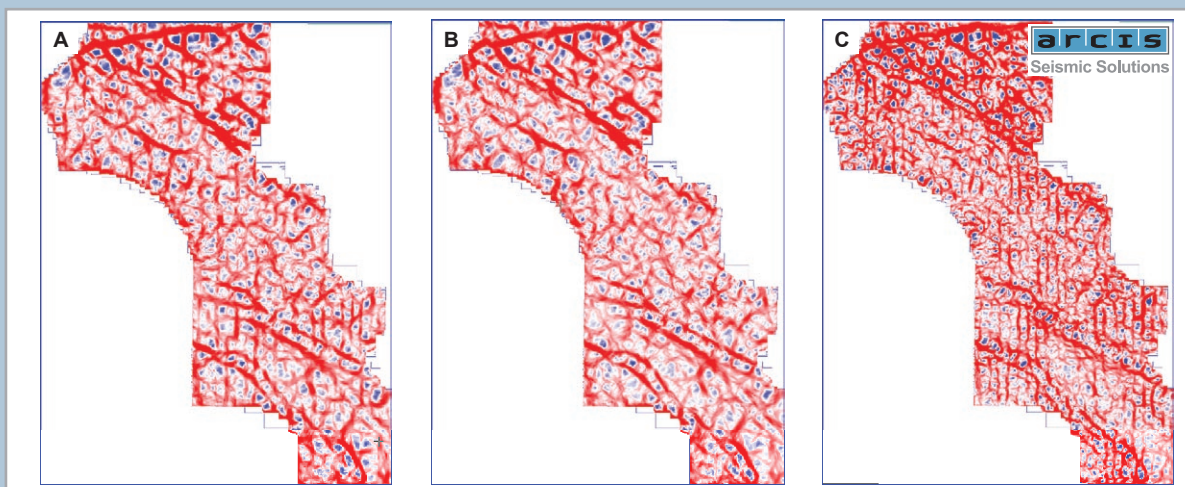


Chair displays with a seismic inline as the vertical display and horizon slices from (A) coherence, (B) most-positive curvature (long-wavelength), (C) most-negative curvature (long-wavelength), (D) most positive curvature (short-wavelength), (E) most-negative curvature (short-wavelength) volumes.



FIGURE 10: COHERENCE/CURVATURE ATTRIBUTE COMPARISON

From ARCIS

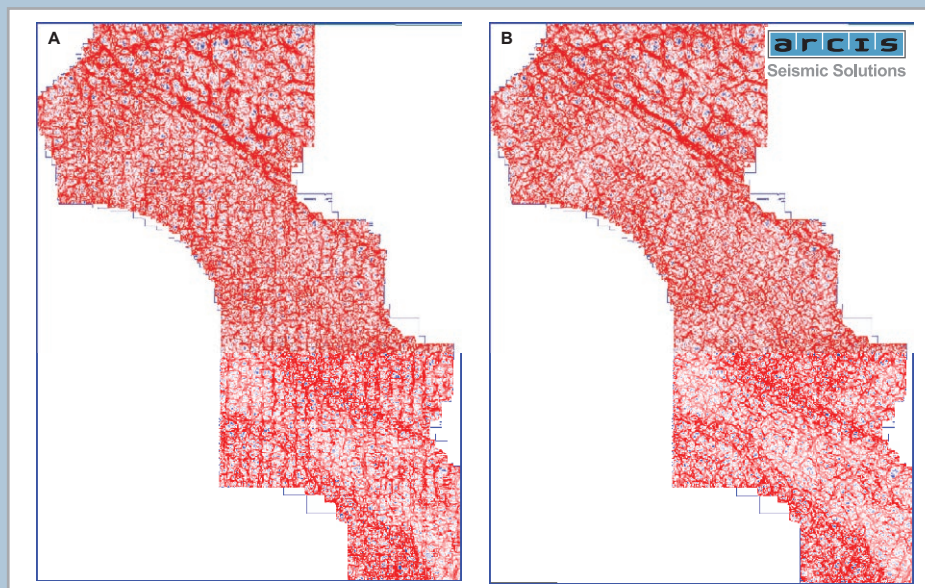


Time slices from (A) Most positive curvature (long-wavelength) run on input data, (note the N-S/amplitude trends reflecting the acquisition geometry). (B) Most positive curvature (long-wavelength) run on input data after footprint filtering. (C) Most positive curvature (intermediate-wavelength) run on input data. Notice, how the removal of the footprint leaves the curvature slice clear of any noise contamination and more amenable for interpretation.



FIGURE 11: SUPPRESSION OF FOOTPRINT AND ATTRIBUTES

From ARCIS

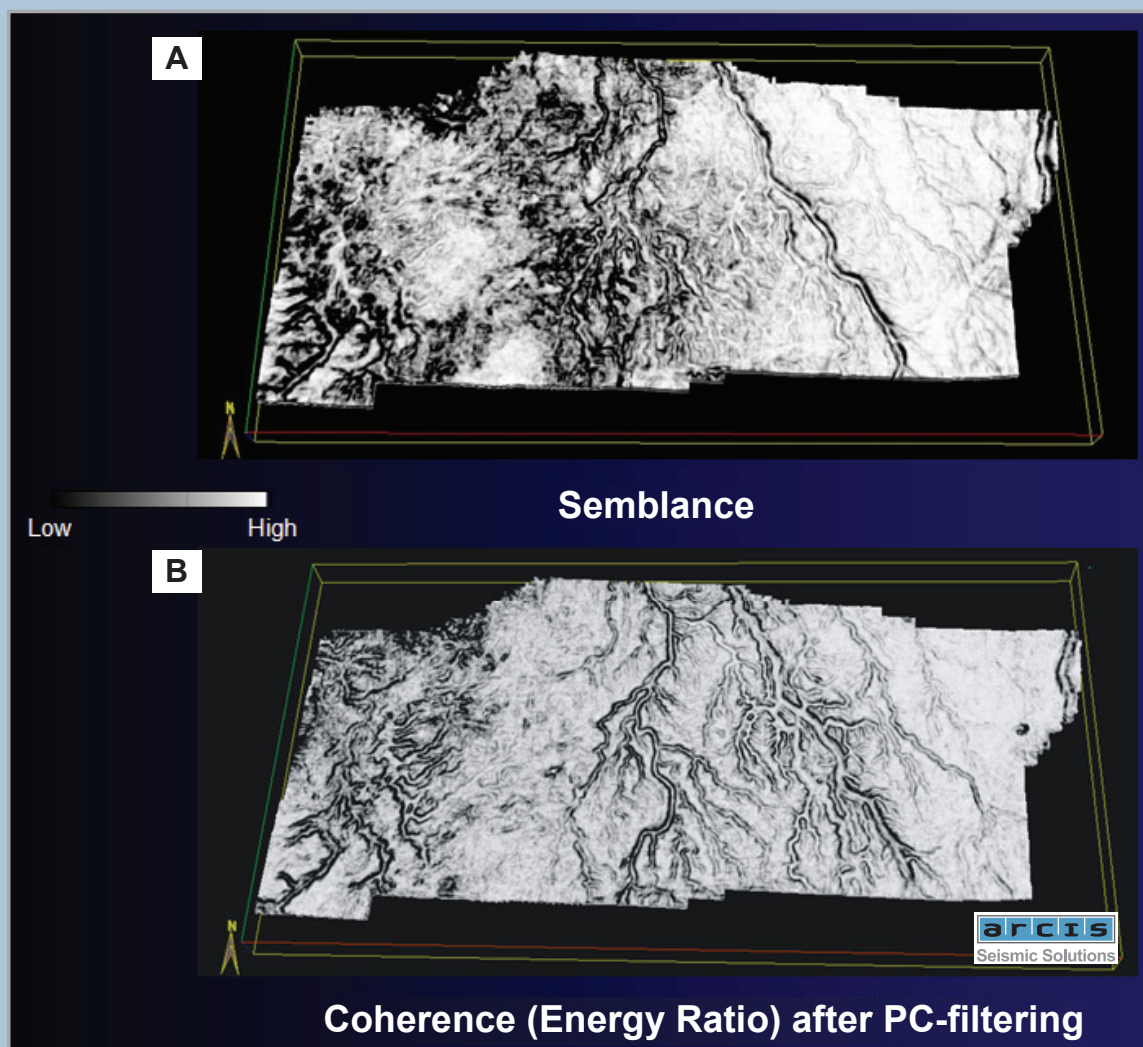


Time slices from (A) Most positive curvature (short-wavelength) run on input data (note the N-S amplitude trends reflecting the acquisition geometry, (B) Most positive curvature (short-wavelength) run on input data after footprint filtering.



FIGURE 12: SUPPRESSION OF FOOTPRINT AND ATTRIBUTES

From ARCIS



Horizon slices through coherence volumes computed (A) using a semblance algorithm from the input data, and (B) using an energy-ratio coherence algorithm from pfiltered seismic data. (Data courtesy: Arcis Corporation, Calgary)



FIGURE 13: EXTRACTING MORE WITH COHERENCE

From ARCIS

picking of peaks and troughs. Once these values are assigned to every data point in the 3D volume, adjacent samples are used to compute volumetric estimates of curvature.

These curvature computations can be made at different scales. Short wavelengths correspond to intense, but highly localized fracture systems, and longer wavelengths to a wider and more even distribution of fractures. Short-wavelength estimates of curvature may incorporate dip information of

9-25 traces, while long-wavelength estimates of curvature may use dip information of 400 or more traces. Various wavelength curvatures are computed along each time slice with dip components previously estimated at each seismic bin. Volume curvature estimates eliminate interpretation problems and allow curvature measurements to be extracted on time slices as well as along horizons enabling local faults and flexures to be mapped where there is no consistent horizon to pick.

Figure 9 (▶ page 25) shows a comparison of time slices from the coherence and the long-wavelength most-positive and most-negative curvature attributes. Clearly, the lineaments seen on the two curvature attributes have more detail than the coherence attribute. To ascertain that each of the lineaments are meaningful, these are usually correlated with the seismic data. Figure 10 (▶ page 26) shows chair displays for coherence and both the long- and short-wavelength displays of most-positive and most-negative curvature horizon slices. While the lineaments seen on the positive curvature (red) indicate the upthrown side of the individual fault blocks, the negative curvature (blue) lineaments indicate the downthrown sides of the fault blocks, and each of these lineaments correlates well with the corresponding seismic signatures.

Figure 11a (▶ page 27) shows time slices from the most-positive curvature (long-wavelength) run on the input data. Notice how the N-S lineaments coming from the acquisition footprint are seen prominently and would interfere with any attempt to interpret lineaments corresponding to geologic features. Figure 11b (▶ page 27) shows the equivalent slice from most-positive curvature computed on input seismic data after footprint filtering. Notice the removal of the vertical imprint. Figure 11c (▶ page 27), shows the equivalent slice from the most-positive curvature run on the input data at intermediate wavelength and the footprint becomes really prominent.

Figure 12 (▶ page 27) shows a similar comparison for the short-wavelength version of most-positive curvature before and after footprint filtering on input data. Again the removal of the footprint can be seen clearly.

Examples of attributes computed on conventional pre-stack time-migrated data volumes before and after noise suppression and frequency bandwidth enhancement are illustrated in figure 13 (▶ opposite page), which shows a comparison between a conventional semblance horizon slice from northeastern British Columbia, Canada and the equivalent slice from the dip-steered energy-ratio coherence volume run on pc-filtered data, using similar lateral and temporal attribute analysis parameters. Notice the clear definition of the main channel, running almost north-south, as well as the branching channels on the west side of the image.

Figure 14 (▶ below) shows stratal slices through attributes computed from both the original and frequency-enhanced data. Note that the improved frequency resolution does not significantly change the long-wavelength curvature. In contrast, the impact on coherence is significant, where increased lateral resolution of the channel system is noted.

Conclusions

With the help of examples, it is shown that computation of attributes is more than a process that involves pressing

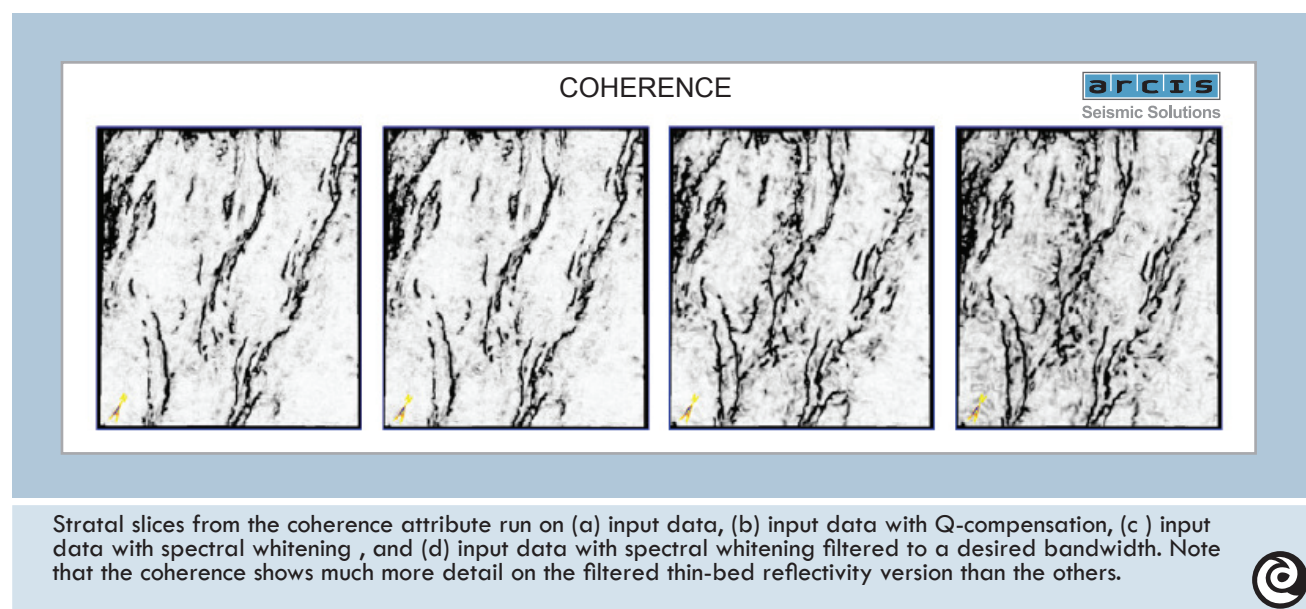


FIGURE 14: COHERENCE ON FREQUENCY-ENHANCED SEISMIC DATA

From ARCIS

some buttons on a workstation. Rather, careful examination of the input seismic data in terms of frequency content as well as signal-to-noise ratio or any other noise contaminating the data is recommended. Structure-oriented filtering can sharpen edges of both structural and stratigraphic features of interest. Frequency enhancement techniques including Q-compensation, spectral whitening, frequency-split structure-oriented filtering and thin-bed reflectivity inversion (in that order) can significantly enhance the frequency content of

seismic data, resulting in more meaningful attribute images. Needless to mention, all these methods may not be available to an interpreter. However, this exercise serves to bring out the information that should be borne in mind while making choices for methods of frequency enhancement. Ideally, all of these tools should be in the hands of the interpreter to allow him to make choices appropriate to the geological hypothesis that he wishes to evaluate.

acknowledgements

I wish to thank Somanath Misra for his help with conditioning of data for some of the examples shown in this paper. I would also like to thank Arcis Corporation for encouraging this work and for permission to publish it.

selected references

Chopra, S., J. Castagna, and O. Portniaguine, 2006, Seismic resolution and thin-bed reflectivity inversion: CSEG Recorder, no. 1, 19-25.

Chopra, S., and K. J. Marfurt, 2007, Seismic Attributes for Prospect Identification and Reservoir

Characterization: SEG.

Chopra, S., and K. J. Marfurt, 2008a, Emerging and future trends in seismic attributes: The Leading Edge, 27, no. 3, 298–318, doi:10.1190/1.2896620.

Chopra, S. and Marfurt, K.J., 2008b, Gleaning meaningful information from seismic attributes: First Break, 43-53.

Gulunay, N., N. Benjamin, and M. Magesan, 2006, Acquisition footprint suppression on 3D land surveys : First Break, 24, no. 2, 71–77.

Helmore, S., 2009, Dealing with the noise-Improving seismic whitening and seismic inversion workflows using frequency split structurally oriented filters, 3367-3371.

Höecker, C., and G. Fehmers, 2002, Fast structural interpretation with structure-oriented filtering: The Leading Edge, 21, no. 3, 238–243, doi:10.1190/1.1463775.

Luo, Y., S. Al-Dossary, and M. Alfaraj, 2002, Acquisition Processing—Edge-preserving smoothing and applications : The Leading Edge, 21, no. 2, 136–158, doi:10.1190/1.1452603.

Marfurt, K. J., 2006, Robust estimates of 3D reflector dip and azimuth: Geophysics, 71, no. 4, P29–P40, doi:10.1190/1.2213049.

Yilmaz, O., 2001, Seismic Data Analysis: Processing, Inversion and Interpretation of Seismic Data, SEG Publication.